

Chiral Waveguide Optomechanics: First Order Quantum Phase Transitions with \mathbb{Z}_3 Symmetry Breaking

D. D. Sedov,¹ V. K. Kozin,^{2,1} and I. V. Iorsh¹

¹*Department of Physics and Engineering, ITMO University, Saint Petersburg 197101, Russia*

²*Science Institute, University of Iceland, Dunhagi-3, IS-107 Reykjavik, Iceland*



(Received 8 September 2020; accepted 9 December 2020; published 31 December 2020)

We present a direct mapping between the quantum optomechanical problem of the atoms harmonically trapped in the vicinity of a chiral waveguide and a generalized quantum Rabi model, and we discuss the analogy between the self-organization of atomic chains in photonic structures and Dicke-like quantum phase transitions in the ultrastrong coupling regime. We extend the class of the superradiant phase transitions for the systems possessing \mathbb{Z}_3 rather than parity \mathbb{Z}_2 symmetry and demonstrate the emergence of the multicomponent Schrödinger-cat ground states in these systems.

DOI: [10.1103/PhysRevLett.125.263606](https://doi.org/10.1103/PhysRevLett.125.263606)

The arrays of quantum emitters coupled to a common one-dimensional photonic reservoir are the main object studied by the emerging field of waveguide quantum electrodynamics (WQED) [1,2]. The field currently experiences a rapid progress due to developments in quantum technologies allowing realizations of this type of system based on a variety of platforms including superconducting qubits [3,4], cold atoms [5], or semiconductor quantum dots [6]. The key features of waveguide quantum optical setups are the emergent long-range correlations between the qubits harnessed through the exchange of the propagating waveguide photons and the inherent open nature of these systems provided by the leakage of the photons. Recently, the setups comprising the ring-shaped topological waveguides have been suggested [7,8], which combine the long-range interqubit correlations and quasi-hermiticity. These setups could be particularly useful for the emulation of the strongly correlated quantum models since the latter are usually Hermitian ones.

One of the factors limiting the diversity of the quantum many-body phenomena supported by the WQED setups is the relatively small radiative coupling of the individual qubits to the photonic mode as compared to the transition frequencies. This leaves us in the weak coupling region of the light-matter interaction. At the same time, reaching the regime of the ultrastrong coupling [9,10] at which the coupling strength becomes comparable with the transition frequencies would enable the access to a plethora of fascinating quantum phenomena such as nonvacuum and correlated ground states, as well as possible application in quantum memory [11] and quantum metrology [12,13]. Also, it turns out that the emergence of superradiant phases is a general property of the ultrastrong coupling limit [14].

In this Letter, we show that the consideration of the atomic mechanical degree of freedom opens the route toward the realization of the ultrastrong coupling regime

in the WQED structures. While the joint dynamics of mechanical and internal degrees of freedom has been considered previously, the analysis relied on the approximations of either classical dynamics of both positions and polarizations of atoms [15] or the truncated Hilbert space for the phonons [16]. In this Letter, we provide a rigorous mapping from the optomechanical problem to the quantum Rabi model and show that the self-organization of atoms predicted in the classical picture corresponds to the Rabi-like phase transition known to appear in the ultrastrong coupling regime. Since there has recently been tremendous progress in finding analytical solutions of the Rabi model [17], we believe that the presented mapping is of substantial importance for the further developments of the quantum optomechanics in the regime of strong optomechanical coupling.

We consider the system depicted in Fig. 1: N qubits are placed in the laser harmonic traps on top of the chiral ring

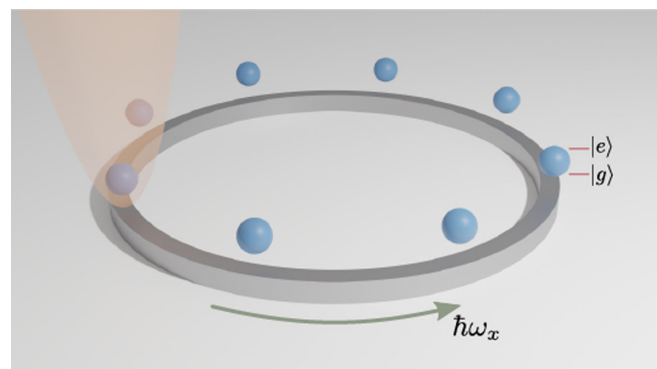


FIG. 1. Geometry of the structure: an array of two-level atoms placed in the vicinity of the chiral ring resonator. The parabolic trapping potential is shown with a shaded region only for one atom.

resonator. The qubit can absorb or emit a waveguide photon, and the radiative relaxation to the far field is suppressed. The Hamiltonian of the system reads

$$\hat{H} = \sum_k \omega_k \hat{c}_k^\dagger \hat{c}_k + \sum_{j=1}^N \omega_x \sigma_j^+ \sigma_j + \sum_{j=1}^N \Omega \hat{a}_j^\dagger \hat{a}_j + \hat{H}_{\text{int}}, \quad (1)$$

where $\omega_k = vk$ is the dispersion of the chiral waveguide modes that is assumed to be linear, v is the speed of light in the waveguide, ω_x is the qubit resonance frequency, and Ω is the optical trap phonon energy; \hat{a}_j and \hat{a}_j^\dagger are annihilation and creation phonon operators, respectively. The interaction Hamiltonian reads

$$\hat{H}_{\text{int}} = g \sum_{k,j} [\sigma_j^\dagger \hat{c}_k e^{ik[R\phi_j + x_j]} + \text{H.c.}], \quad (2)$$

where g is the Rabi splitting; R is the radius of the ring; x_j corresponds to the deviation of the j th atom from its equilibrium position, which is equal to $u_0(\hat{a}_j + \hat{a}_j^\dagger)$; and $u_0 = \sqrt{\hbar/(2M\Omega)}$ is the quantum of the mechanical motion, where M is the mass of the qubit. Actually, the optical spectrum of the ring is discrete rather than continuous, with the frequency difference between the modes given by $\delta\omega = v/R$. However, for a large resonator when $v/R \ll \omega_x$, the limit of the continuous spectrum can be employed.

We then integrate out the waveguide degrees of freedom by performing the Schrieffer-Wolff transform [18] to obtain the effective Hamiltonian up to the second order of the qubit-photon coupling g :

$$\begin{aligned} \hat{H}_{\text{eff}} = & \sum_j \omega_x \sigma_j^+ \sigma_j + \sum_j \Omega \hat{a}_j^\dagger \hat{a}_j \\ & - \frac{\Gamma_0}{2} \sum_{i < j} [i \sigma_i^+ \sigma_j e^{iqR\phi_{ij}} e^{i\eta(\hat{a}_i + \hat{a}_i^\dagger - \hat{a}_j - \hat{a}_j^\dagger)} + \text{H.c.}], \end{aligned} \quad (3)$$

where $q = \omega_x/v$, $\Gamma_0 = g^2/v$ is the radiative decay rate of a single qubit, and $\eta = qu_0$ is the dimensionless optomechanical interaction. In deriving Eq. (3), we used the Markov approximation, neglecting the frequency dispersion in the phase factor ($k \approx q$). The Markov approximation holds for $R\Gamma_0/v \ll 1$. In stark contrast to the WQED case, the resulting Hamiltonian is Hermitian. This is both due to the fact that, unlike the case of an infinite waveguide, our system is a closed one and because the radiation to the far field has been neglected. The latter approximation can be adopted when the radiative coupling to the waveguide mode Γ_0 is much stronger than that to the far-field continuum Γ' . This can be achieved in the photonic crystal waveguide geometries, where $\Gamma_0/\Gamma' > 9$ has been experimentally reported [19].

The qubit excitation energy ω_x is the largest energy scale of the problem. Since the Hamiltonian commutes with the

excitation number operator, we can safely project the Hamiltonian to the subspace with a single excitation. In this case, the qubit subspace is spanned by N states corresponding to excitation localized at each of the N qubits. We assume the equidistant spacing of the harmonic traps, i.e., $\phi_{i+1,i} = \phi$.

The third term in Eq. (3) contains the exponent of the bosonic operators, making it highly nonlinear in the region $\eta \approx 1$. It is instructive to estimate the experimentally relevant range of parameters of the model. Parameter η is defined by the ratio of the length scale of the atomic motion u_0 and the wavelength of the photon in the waveguide λ : $\eta = 4\pi u_0/\lambda$. The coherence of the atomic motion is preserved at the scale of the atomic de Broglie wavelength $\lambda = \hbar/p_{\text{th}}$, where the thermal momentum $p_{\text{th}} = \sqrt{3Mk_B T}$. Thus, the condition of the coherent atomic motion implies that $u_0 < \hbar/p_{\text{th}}$. For the lithium atoms and the resonant wavelength of approximately 700 nm, the value of $\eta = 1$ is achieved at $T = 640$ nK, which is a temperature that has been achieved in recent cold-atom experiments (see the review [20] and references within). The corresponding phonon energy is then approximately 2.4 kHz. The radiative decay rate Γ_0 can be tuned in a wide range of frequencies from zero to the gigahertz. Therefore, the range of Γ_0/Ω , $\eta \sim 1$ can be achieved in the state of the art cold-atom experiments. Thus, it is relevant to explore the properties of the Hamiltonian [Eq. (3)] outside the small η regime.

We introduce the unitary transformation T_N for the case of N qubits, which transforms Eq. (3) to a more familiar form. The general expression for T_N can be found in Supplemental Material [21]. For the case of two qubits, T_2 reads $\hat{T} \hat{H}_{\text{eff}} \hat{T}^\dagger$, where

$$T = \frac{1}{\sqrt{2}} \begin{pmatrix} i e^{-i\eta \hat{x}_1} & e^{-i\eta \hat{x}_2 - iqR\phi} \\ -i e^{i\eta \hat{x}_1} & e^{-i\eta \hat{x}_2 - iqR\phi} \end{pmatrix}, \quad (4)$$

where $\hat{x}_i = \hat{a}_i + \hat{a}_i^\dagger$, and the transformed Hamiltonian

$$\begin{aligned} \hat{T}_2 \hat{H}_{\text{eff}} \hat{T}_2^\dagger = & \Omega \left[\hat{a}_{\text{CM}}^\dagger \hat{a}_{\text{CM}} + \hat{a}_d^\dagger \hat{a}_d + \frac{\eta^2}{2} \right. \\ & \left. + \sigma_x \frac{\eta}{\sqrt{2}} (i \hat{a}_d - i \hat{a}_d^\dagger) - \frac{\Gamma_0}{2\Omega} \sigma_z \right], \end{aligned} \quad (5)$$

$\hat{a}_{\text{CM}} = (1/\sqrt{2})(\hat{a}_1 + \hat{a}_2 + i\eta)$ corresponds to the center-of-mass qubit motion, and $\hat{a}_d = 1/\sqrt{2}(\hat{a}_1 - \hat{a}_2)$ corresponds to the relative motion of two qubits. The center-of-mass momentum operator is shifted from the equilibrium position on η . This is due to the unidirectional propagation of the chiral waveguide photon, which *pushes* the qubits as a whole in one direction. Then, we see that the spectrum of the problem does not depend on the static phase difference ϕ , which is typical for the chiral waveguide quantum optical setups [22,23]. Finally, we see that up to the center-of-mass kinetic energy term, which

decouples from the rest of the system, the effective Hamiltonian is exactly the one corresponding to the quantum Rabi model. The radiative decay Γ_0 plays the role of the resonant transition energy, and the η defines the effective coupling strength. The case of strong optomechanical interaction $\eta > 0.1\sqrt{2}$ thus directly maps to the ultrastrong coupling (USC) regime. It is known that in the USC and deep-strong coupling regimes ($\eta > \sqrt{2}$) of the Rabi model, the system is characterized by the nonvacuum ground state $|\Psi_G\rangle$, which can be roughly approximated by the superposition of the coherent states [24]

$$|\Psi_G\rangle \approx \frac{1}{\sqrt{2}}(|+\rangle \otimes |\alpha\rangle + |-\rangle \otimes |-\alpha\rangle),$$

where $|\pm\alpha\rangle$ are the bosonic coherent states, and $|\pm\rangle = 1/\sqrt{2}(|\uparrow\rangle \pm |\downarrow\rangle)$ are the superpositions of the ground and excited qubit states. Also, the direct mapping to the Rabi model is valid only in the purely chiral case. However, as we show in the Supplemental Material (SM) [21], the numerically obtained spectrum for the nonperfectly chiral waveguide is qualitatively very similar to the perfectly chiral case.

For three qubits, the unitary transformation T_3 results in the Hamiltonian [21]

$$\hat{T}_3 \hat{H}_{\text{eff}} \hat{T}_3^\dagger = \hat{H}_{\text{eff}} = \hat{H}_{\text{ph}} + \hat{H}_q + \hat{H}_c, \quad (6)$$

where \hat{H}_{ph} is the phonon kinetic energy given by

$$\hat{H}_{\text{ph}} = \Omega \left(\hat{a}^\dagger \hat{a} + \hat{a}_x^\dagger \hat{a}_x + \hat{a}_y^\dagger \hat{a}_y + \frac{2\eta^2}{3} \right), \quad (7)$$

where \hat{a} corresponds to the shifted operator of the center-of-mass motion, $\hat{a} = 1/\sqrt{3}(\hat{a}_1 + \hat{a}_2 + \hat{a}_3 + i\eta)$, and $\hat{a}_x = 1/\sqrt{6}(-\hat{a}_1 - \hat{a}_2 + 2\hat{a}_3)$ and $\hat{a}_y = 1/\sqrt{2}(\hat{a}_1 - \hat{a}_2)$ are operators of normal modes. The qubit Hamiltonian \hat{H}_q reads

$$\hat{H}_q = -\frac{\sqrt{3}\Gamma_0}{2} \hat{\lambda}_3, \quad (8)$$

where $\hat{\lambda}_i$ is the 3×3 Gell-Mann matrix. Finally, the coupling term \hat{H}_c reads

$$\hat{H}_c = -\frac{\Omega\eta}{\sqrt{3}} [\hat{p}_x(\hat{\lambda}_1 + \hat{\lambda}_4 + \hat{\lambda}_6) + \hat{p}_y(-\hat{\lambda}_2 + \hat{\lambda}_5 - \hat{\lambda}_7)], \quad (9)$$

where $\hat{p}_i = i/\sqrt{2}(\hat{a}_i - \hat{a}_i^\dagger)$. The Hamiltonian \hat{H}_{eff} (up to the decoupled center-of-mass motion) describes the two-dimensional Bose-Einstein condensate (BEC) of spin 1 particles localized in a harmonic trap (given by \hat{H}_{ph}) and in a perpendicular magnetic field \hat{H}_q . The term \hat{H}_c describes the spin-orbit coupling (SOC) for spin 1 particles. This type of SOC has been introduced for the BECs of spin particles previously [25,26]. Thus, we highlight a link between the waveguide optomechanical systems and BEC physics.

Despite seeming similarity, the Hamiltonian in Eq. (6) is qualitatively different from the Dicke model Hamiltonian. Namely, the qubit operators do not obey the angular momentum commutation relations. Moreover, the Hamiltonian [Eq. (6)] possesses global \mathbb{Z}_3 symmetry. Consider the unitary operator

$$\hat{R} = e^{-i\hat{L}_z(2\pi/3)} \otimes \begin{pmatrix} 1 & 0 & 0 \\ 0 & e^{i4\pi/3} & 0 \\ 0 & 0 & e^{i2\pi/3} \end{pmatrix}, \quad (10)$$

where $\hat{L}_z = \hat{x}\hat{p}_y - \hat{y}\hat{p}_x$ is the angular momentum operator. Operator \hat{R} obeys $\hat{R}^2 = \hat{R}^\dagger$, and thus $[1, \hat{R}, \hat{R}^2]$ form a group. We note that $\hat{R}\hat{H}_{\text{eff}}\hat{R}^\dagger = \hat{H}_{\text{eff}}$, and thus $[\hat{R}, \hat{H}_{\text{eff}}] = 0$. Therefore, the eigenstates of \hat{R} are also eigenstates of \hat{H}_{eff} . The three distinct eigenvalues of \hat{R} are $[1, e^{i2\pi/3}, e^{i4\pi/3}]$.

We then assume the limit of the classical motion of the qubits by assuming \hat{p}_x and \hat{p}_y to be classical variables; and we find the eigenvalues of the corresponding matrix Hamiltonian obtained from Eq. (6). We find the ground state energy by minimizing the smallest eigenvalue with respect to p_x and p_y . Moving to the polar coordinates $(p_x, p_y) = (p \cos \theta, p \sin \theta)$, we find that the minimum energy is obtained for $\cos 3\theta = 1$. With this condition fulfilled, the expression for the ground state energy as a function of p reads

$$\epsilon_G = \frac{2\eta^2\Omega}{3} + \frac{\sqrt{3}\Gamma_0}{2} \left[\frac{\tilde{p}^2}{2\mu} - 2 \left(\tilde{p}^2 + \frac{1}{3} \right)^{1/2} \cos\left(\frac{\gamma}{3}\right) \right], \quad (11)$$

where $\mu = \sqrt{4/27}\eta^2\Omega/\Gamma_0$, $\tilde{p} = 2\eta\Omega/(3\Gamma_0)p$, and $\gamma = \arctan[(81\tilde{p}^4 + 27\tilde{p}^2 + 3)^{1/2}/9\tilde{p}^3]$. For small \tilde{p} , we can write

$$\epsilon_G \approx \frac{2\eta^2\Omega}{3} + \frac{\sqrt{3}\Gamma_0}{2} \left[-1 - \tilde{p}^3 + \frac{9\tilde{p}^4}{8} + \frac{\mu-3}{2\mu} \tilde{p}^2 \right]. \quad (12)$$

For $\eta \ll 1$, Eq. (12) has a single local minimum at $\tilde{p} = 0$.

For $\eta > \eta_c = \sqrt{3\sqrt{3}\Gamma_0/(7\Omega)}$, it has an additional minimum at \tilde{p}_c , which for $\eta \approx \eta_c$ can be approximated by $\tilde{p}_c \approx (1/3)(1 + \sqrt{7-2/\mu})$. Then, for $\eta > \sqrt{\sqrt{3}\Gamma_0/(2\Omega)}$, there is only a single minimum at \tilde{p}_c . At $\eta = \eta_c$, the first derivative of ϵ_G is discontinuous, which is a hallmark of the first order quantum phase transition [27].

We plot the dependence of ϵ_G given by Eq. (11) in Fig. 2(a). We can see that, indeed, there exists a range of parameters where there are two local minima signifying the phase coexistence regime. Thus, the quantum phase transition (QPT) in the classical limit is indeed of the first order. This is in stark contrast to the classical limit of the quantum Rabi model, where the phase transition is of the second order [28].

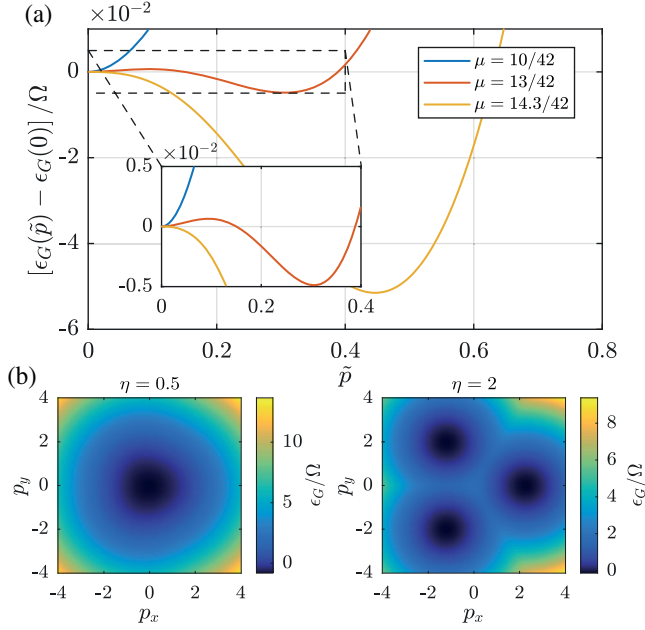


FIG. 2. (a) Dependency of the ground state energy on \tilde{p} for different values of the parameter μ ; $\Gamma_0/\Omega = 2.5$. (b) Dispersion of the lowest energy surface in the classical approximation for qubit motion in the two cases: $\eta = 0.5$ and $\eta = 2.0$; $\Gamma_0/\Omega = 2.5$, and $\eta_c \approx 1.36$.

The map of the ϵ_G in (p_x, p_y) space is shown in Fig. 2(b). For the case of $\eta < \eta_c$ shown in the left panel, there is a single minimum corresponding to $\tilde{p} = 0$. For the $\eta > \eta_c$ (right) panel, three degenerate minima emerge.

Since the QPTs can occur only in the thermodynamic limit, we shall refine our analysis of the ground state energy. For that, we first consider that the actual quantum states corresponding to the minimal energy in the classical limit are the direct products of the spin states and the coherent states of the qubit motion at small p_c :

$$|l\rangle \approx \mathcal{N}_c \left(\begin{array}{c} \frac{\tilde{p}_c}{2} \\ - \left[1 - \frac{5}{8} \tilde{p}_c^2 \right] e^{2i\theta_l} \\ \tilde{p}_c e^{i\theta_l} \end{array} \right) \otimes |\tilde{p}_c \cos \theta_l, \tilde{p}_c \sin \theta_l\rangle, \quad (13)$$

where $l = 0, 1, 2$; $\theta_l = 2\pi l/3$; and \mathcal{N}_c is the normalization factor. It is evident that $\langle l | \hat{H}_{\text{eff}} | l \rangle$ yields the classical mean-field ground state energy. However, these states cannot be the eigenstates of Hamiltonian \hat{H}_{eff} since they are not eigenstates of operator \hat{R} . Namely, $\hat{R}|l\rangle = |[(l+1) \bmod 3]\rangle$. Moreover, due to nonorthogonality of the coherent states, $\langle l' | \hat{H}_{\text{eff}} | l \rangle \neq E \delta_{l',l}$ and $\langle l' | l \rangle \neq \delta_{l',l}$. We thus can solve the characteristic equation for the eigenvalues $\det[\langle l' | \hat{H}_{\text{eff}} | l \rangle - E \langle l' | l \rangle] = 0$. The explicit form of the characteristic equation is cumbersome and presented in the Supplemental Material [21]. However, the nondiagonal

elements of the matrix representation of the Hamiltonian are proportional to the overlap of the coherent states, which is proportional to $\exp[-3\tilde{p}_c^2]$. The explicit form of the eigenstates can be found from the symmetry considerations. Namely, the eigenstates should also be the eigenstates of the operator \hat{R} . We then can easily find the mutually orthogonal linear superpositions of states $|l\rangle$ that satisfy this condition. Namely, the ground and two excited states are given by

$$\begin{aligned} |\Psi_G\rangle &= \frac{1}{\sqrt{3}} [|0\rangle + |1\rangle + |2\rangle], \\ |\Psi_{E1}\rangle &= \frac{1}{\sqrt{3}} [|0\rangle + e^{4i\pi/3}|1\rangle + e^{2i\pi/3}|2\rangle], \\ |\Psi_{E2}\rangle &= \frac{1}{\sqrt{3}} [|0\rangle + e^{2i\pi/3}|1\rangle + e^{4i\pi/3}|2\rangle]. \end{aligned} \quad (14)$$

The spectrum of \hat{H}_{eff} as a function of the coupling strength η is shown in Fig. 3 for the case of the ground state of the center-of-mass degree of freedom $\hat{n}_{\text{CM}} = 0$. The spectrum has been obtained via the direct numerical diagonalization by truncating the phonon subspace. We can see that at large η , the ground state becomes quasidegenerate. We also plot the analytically obtained dispersions of states $|\Psi_G\rangle$, $|\Psi_{E1}\rangle$, and $|\Psi_{E2}\rangle$. The first three low energy states given by Eq. (14) are the analog of the triangular Schrödinger-cat states [29]. While the Schrödinger-cat states are generally regarded as extremely fragile with respect to decoherence, it has been recently revealed that the two-component cat states appearing in the USC of the conventional Rabi model appear to be robust to decoherence and can be used to realize protected quantum gates with high fidelity [30,31]. Thus, the states $|\Psi_{[G,E1,E2]}\rangle$ as the three-component generalizations of the cat states

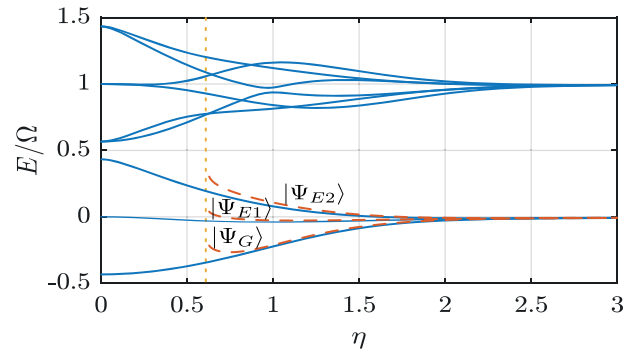


FIG. 3. Eigenenergies of first nine eigenstates of \hat{H}_{eff} vs optomechanical coupling η with $\Gamma_0/\Omega = 0.5$. Red dashed lines show the dispersions of states in Eq. (14), and blue solid lines show the results of the numerical diagonalization. The vertical dotted line corresponds to critical optomechanical coupling $\eta_c \approx 0.61$. For the numerical diagonalization, the phonon subspace was truncated with a maximal phonon occupation number of 100.

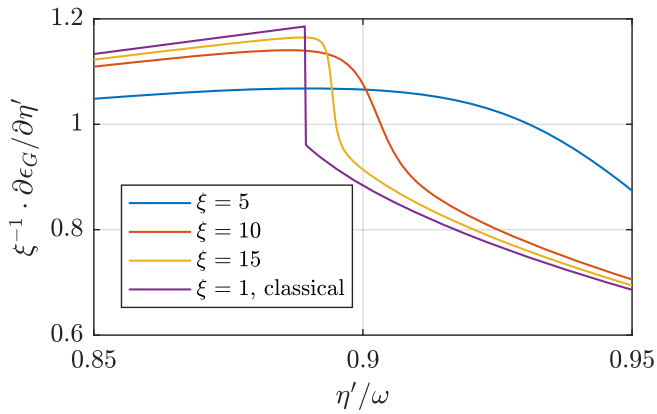


FIG. 4. First derivative of the ground state energy $\partial \epsilon_G / \partial \eta'$ for different values of scaling parameter ξ : $\omega = 1$.

originating in the USC are likely to remain sufficiently stable and can be used for quantum information processing.

We have shown that the phase transition occurs in the classical limit. The classical limit can be regarded as a thermodynamic limit of the vanishing harmonic oscillator energy Ω [28,32–34]. To explore this limit, we redefine the energy constants in \hat{H}_{eff} in the following way: we set $\eta\Omega \rightarrow \eta'$ as an independent variable and redefine $\Gamma_0 = \xi\omega$ and $\Omega = \omega/\xi$. The thermodynamic limit is then achieved for $\xi \rightarrow \infty$.

In Fig. 4, we plot the first derivative of the ground state energy as a function of η' for $\omega = 1$ and for different ξ . As ξ increases, this function steepens in the vicinity of η'_c . In the limit of infinite ξ , we would observe the discontinuity of the $\partial \epsilon_G / \partial \eta'$ just as in the classical limit and the establishment of the QPT with \mathbb{Z}_3 symmetry breaking. The $\Omega \rightarrow 0$ limit can be regarded as the classical limit of the atomic motion. Thus, the predicted phase transition corresponds to the appearance of non-zero phonon occupation in the ground state and self-organization of atomic motion due to the photon mediated inter-atomic interactions. The self-organization of atoms has been predicted within the classical approach in WQED systems [15]. We thus reveal the direct connection of the self-organization phenomena and quantum phase transitions similar to that occurring in the Rabi model.

To conclude, we have established a direct mapping between the quantum optomechanical setup in the chiral waveguide and the generalization of the quantum Rabi model. Whereas for two qubits, the system directly maps to the quantum Rabi model; already for the case of three qubits, the system possesses unconventional \mathbb{Z}_3 symmetry, exhibiting multicomponent Schrödinger-cat ground states as well as \mathbb{Z}_3 symmetry breaking first order phase transitions in the thermodynamic limit. The work establishes solid connections between the self-organization of atoms in photonic structures, which has been previously treated, and quantum phase transitions. It also poses an interesting question on the structure of the ground state in the limit of

the large number of qubits N . While we have demonstrated the \mathbb{Z}_N symmetry for N qubits (see SM), the nature of the phase transition and the structure of the ground state are yet to be explored.

The results of the Letter can be applied to a more general class of systems of moving atoms in the photonic structures since they reveal that the apparatus developed in the studies of the USC can be directly applied to explore both fundamental aspects of quantized spin-motion coupling and perspective applications in quantum information processing.

The work of Ivan Iorsh (mapping to the Rabi model) was supported by the Russian Science Foundation (project 20-12-00224). The work of Denis Sedov (numerical solution of three qubit model) was supported by Russian Science Foundation (project 20-12-00194). We thank A. N. Poddubny, A. V. Poshakinskiy, and M. I. Petrov for fruitful discussions.

-
- [1] D. Roy, C. M. Wilson, and O. Firstenberg, *Rev. Mod. Phys.* **89**, 021001 (2017).
 - [2] D. E. Chang, J. S. Douglas, A. González-Tudela, C.-L. Hung, and H. J. Kimble, *Rev. Mod. Phys.* **90**, 031002 (2018).
 - [3] A. F. van Loo, A. Fedorov, K. Lalumiere, B. C. Sanders, A. Blais, and A. Wallraff, *Science* **342**, 1494 (2013).
 - [4] M. Mirhosseini, E. Kim, X. Zhang, A. Sipahigil, P. B. Dieterle, A. J. Keller, A. Asenjo-Garcia, D. E. Chang, and O. Painter, *Nature (London)* **569**, 692 (2019).
 - [5] N. V. Corzo, J. Raskop, A. Chandra, A. S. Sheremet, B. Gouraud, and J. Laurat, *Nature (London)* **566**, 359 (2019).
 - [6] A. P. Foster, D. Hallett, I. V. Iorsh, S. J. Sheldon, M. R. Godland, B. Royall, E. Clarke, I. A. Shelykh, A. M. Fox, M. S. Skolnick *et al.*, *Phys. Rev. Lett.* **122**, 173603 (2019).
 - [7] S. Barik, A. Karasahin, S. Mittal, E. Waks, and M. Hafezi, *Phys. Rev. B* **101**, 205303 (2020).
 - [8] M. J. Mehrabad, A. P. Foster, R. Dost, A. M. Fox, M. S. Skolnick, and L. R. Wilson, [arXiv:1912.09943](https://arxiv.org/abs/1912.09943).
 - [9] A. F. Kockum, A. Miranowicz, S. D. Liberato, S. Savasta, and F. Nori, *Nat. Rev. Phys.* **1**, 19 (2019).
 - [10] P. Forn-Díaz, L. Lamata, E. Rico, J. Kono, and E. Solano, *Rev. Mod. Phys.* **91**, 025005 (2019).
 - [11] T. H. Kyaw, S. Felicetti, G. Romero, E. Solano, and L.-C. Kwek, *Sci. Rep.* **5**, 8621 (2015).
 - [12] C. S. Colley, J. C. Hebden, D. T. Delpy, A. D. Cambrey, R. A. Brown, E. A. Zibik, W. H. Ng, L. R. Wilson, and J. W. Cockburn, *Rev. Sci. Instrum.* **78**, 123108 (2007).
 - [13] M. Ruggenthaler, N. Tancogne-Dejean, J. Flick, H. Appel, and A. Rubio, *Nat. Rev. Chem.* **2**, 0118 (2018).
 - [14] S. Felicetti and A. Le Boité, *Phys. Rev. Lett.* **124**, 040404 (2020).
 - [15] D. E. Chang, J. I. Cirac, and H. J. Kimble, *Phys. Rev. Lett.* **110**, 113606 (2013).
 - [16] M. T. Manzoni, L. Mathey, and D. E. Chang, *Nat. Commun.* **8**, 1 (2017).
 - [17] D. Braak, *Phys. Rev. Lett.* **107**, 100401 (2011).

- [18] S. Bravyi, D.P. DiVincenzo, and D. Loss, *Ann. Phys. (Amsterdam)* **326**, 2793 (2011).
- [19] A. P. Burgers, L. S. Peng, J. A. Muniz, A. C. McClung, M. J. Martin, and H. J. Kimble, *Proc. Natl. Acad. Sci. U.S.A.* **116**, 456 (2019).
- [20] J. R. Anglin and W. Ketterle, *Nature (London)* **416**, 211 (2002).
- [21] See Supplemental Material at <http://link.aps.org/supplemental/10.1103/PhysRevLett.125.263606> for details of theoretical calculations.
- [22] M. Pletyukhov and V. Gritsev, *New J. Phys.* **14**, 095028 (2012).
- [23] D. F. Kornovan, M. I. Petrov, and I. V. Iorsh, *Phys. Rev. B* **96**, 115162 (2017).
- [24] C. Emary and T. Brandes, *Phys. Rev. A* **69**, 053804 (2004).
- [25] R. Barnett, G. R. Boyd, and V. Galitski, *Phys. Rev. Lett.* **109**, 235308 (2012).
- [26] W. Han, X.-F. Zhang, S.-W. Song, H. Saito, W. Zhang, W.-M. Liu, and S.-G. Zhang, *Phys. Rev. A* **94**, 033629 (2016).
- [27] S. Sachdev, *Handbook of Magnetism and Advanced Magnetic Materials* (John Wiley & Sons, Ltd, 2007).
- [28] M.-J. Hwang, R. Puebla, and M. B. Plenio, *Phys. Rev. Lett.* **115**, 180404 (2015).
- [29] B. Vlastakis, G. Kirchmair, Z. Leghtas, S. E. Nigg, L. Frunzio, S. M. Girvin, M. Mirrahimi, M. H. Devoret, and R. J. Schoelkopf, *Science* **342**, 607 (2013).
- [30] P. Nataf and C. Ciuti, *Phys. Rev. Lett.* **107**, 190402 (2011).
- [31] Y. Wang, J. Zhang, C. Wu, J. Q. You, and G. Romero, *Phys. Rev. A* **94**, 012328 (2016).
- [32] L. Bakemeier, A. Alvermann, and H. Fehske, *Phys. Rev. A* **85**, 043821 (2012).
- [33] S. Ashhab, *Phys. Rev. A* **87**, 013826 (2013).
- [34] R. Puebla, M.-J. Hwang, J. Casanova, and M. B. Plenio, *Phys. Rev. Lett.* **118**, 073001 (2017).